



# Discovery of an Accretion-rate Independent Absolute RMS Amplitude of Millihertz Quasi-periodic Oscillations in 4U 1636-53

Ming Lyu<sup>1</sup>, Mariano Méndez<sup>2</sup>, D. Altamirano<sup>3</sup>, Guobao Zhang<sup>4,5</sup> , and G. C. Mancuso<sup>6,7,3</sup>

<sup>1</sup> Department of Physics, Xiangtan University, Xiangtan, Hunan 411105, People's Republic of China; [lvming@xtu.edu.cn](mailto:lvming@xtu.edu.cn)

<sup>2</sup> Kapteyn Astronomical Institute, University of Groningen, P.O. Box 800, NL-9700 AV Groningen, The Netherlands

<sup>3</sup> Physics & Astronomy, University of Southampton, Southampton, Hampshire SO17 1BJ, UK

<sup>4</sup> Yunnan Observatories, Chinese Academy of Sciences (CAS), Kunming 650216, People's Republic of China

<sup>5</sup> Key Laboratory for the Structure and Evolution of Celestial Objects, CAS, Kunming 650216, People's Republic of China

<sup>6</sup> Instituto Argentino de Radioastronomía (CCT-La Plata, CONICET; CICPBA), C.C. No. 5, 1894 Villa Elisa, Argentina

<sup>7</sup> Facultad de Ciencias Astronómicas y Geofísicas, Universidad Nacional de La Plata, Paseo del Bosque s/n, 1900 La Plata, Argentina

Received 2019 May 18; revised 2019 September 1; accepted 2019 September 12; published 2019 October 24

## Abstract

We investigate the frequency and amplitude of the millihertz quasi-periodic oscillations (mHz QPOs) in the neutron-star low-mass X-ray binary 4U 1636–53 using *Rossi X-ray Timing Explorer* observations. We find that no mHz QPOs appear when the source is in the hard spectral state. We also find that there is no significant correlation between the frequency and the fractional RMS amplitude of the mHz QPOs. Notwithstanding, for the first time, we find that the absolute rms amplitude of the mHz QPOs is insensitive to the parameter  $S_a$ , which measures the position of the source in the color–color diagram and is usually assumed to be an increasing function of mass accretion rate. This finding indicates that the transition from marginally stable burning to stable burning or unstable burning could happen very rapidly since, before the transition, the mHz QPOs do not gradually decay as the rate further changes.

*Key words:* methods: data analysis – stars: neutron – X-rays: binaries

## 1. Introduction

A unique class of quasi-periodic oscillations (QPOs) was first discovered by Revnivtsev et al. (2001) in three neutron star low-mass X-ray binaries (LMXBs): 4U 1608–52, 4U 1636–53, and Aql X–1. The unique properties of these QPOs are (Revnivtsev et al. 2001; Altamirano et al. 2008b; Lyu et al. 2015): (1) their typical frequency range is very low, about 6–14 mHz; (2) they are stronger at low photon energies (<5 keV); (3) they appear only when the source is within a narrow range of X-ray luminosities,  $L_{2-20 \text{ keV}} \simeq (5-11) \times 10^{36} \text{ erg s}^{-1}$ ; (4) they disappear or become undetectable when there is a type I X-ray burst.

Revnivtsev et al. (2001) proposed that the mHz QPOs originate from a special mode of nuclear burning on the neutron-star surface, when the mass accretion rate is within a certain range. Heger et al. (2007) proposed that the mHz QPOs could be a consequence of marginally stable nuclear burning of helium on the neutron-star surface. In the model of Heger et al. (2007), the characteristic timescale of the oscillations is  $\sim 100 \text{ s}$ , remarkably consistent with the  $\sim 2 \text{ min}$  period of the mHz QPOs. Also, the model predicts that the oscillations should occur only in a very narrow range of X-ray luminosity. However, the marginally stable nuclear burning in the model occurs only when the accretion rate is close to the Eddington rate, one order of magnitude higher than the averaged global rate over the entire neutron-star surface, calculated from the X-ray luminosity at which mHz QPOs are observed. Heger et al. (2007) proposed that the local accretion rate in the burning layer where the QPOs occur can be higher than the global accretion rate.

An anti-correlation between the frequency of a kilohertz (kHz) QPO and the 2–5 keV X-ray count rate associated with a 7.5 mHz QPO has been reported in 4U 1608–52 (Yu & van der Klis 2002). This result supported the nuclear burning

interpretation of the mHz QPOs: as the luminosity increases, the stresses of the radiation from the neutron-star surface push outward the inner disk in each mHz QPO cycle, thus leading to the change of kHz QPO frequency.

Altamirano et al. (2008b) found that, in the transitional state between the soft and hard spectral states, the frequency of the mHz QPO in 4U 1636–53 decreased systematically with time, until the oscillations disappeared and a type I X-ray burst occurred. Very recently, Mancuso et al. (2019) found a similar behavior in the LMXB EXO 0748–676. This frequency drift behavior further supported the idea that mHz QPOs are closely connected to nuclear burning on the neutron-star surface. The discovery of “high-luminosity” mHz QPOs in the neutron-star transient source IGR J17480–2446 (Linares et al. 2010; Chakraborty & Bhattacharyya 2011) indicated that some mHz QPOs appear with different characteristics. The “high-luminosity” QPOs have a frequency of about 4.5 mHz, and the persistent luminosity of this source when the mHz QPOs were observed was  $L_{2-50 \text{ keV}} \sim 10^{38} \text{ erg s}^{-1}$ . Linares et al. (2012) showed that there is a smooth transition between mHz QPO and thermonuclear bursts in IGR J17480–2446: as the accretion rate increased, bursts gradually evolved into a mHz QPO, and vice versa. This evolution is consistent with the prediction from the marginally stable burning model of Heger et al. (2007), further supporting the idea that mHz QPOs are due to marginally stable burning on the neutron-star surface.

Stiele et al. (2016) studied phase-resolved energy spectra of the mHz QPOs in 4U 1636–53 and found that the oscillations were not caused by variations in the blackbody temperature of the neutron-star surface. Conversely, Strohmayer et al. (2018) recently found that the mHz oscillations in the “clocked burster” GS 1826–238 were consistent with being produced by modulation of the temperature component of the blackbody emission from the neutron-star surface, assuming a constant

blackbody normalization throughout the oscillation cycle. This finding favors the model by Heger et al. (2007); however, as emphasized by Strohmayer et al. (2018), given the current data, that is not the only possible interpretation. Therefore, the connection between the mHz oscillations and the variation of the thermal radiation from the neutron-star surface remains an open question.

A scenario considering the turbulent chemical mixing of the fuel, together with a higher heat flux from the crust, is able to explain the observed accretion rate at which mHz QPOs are seen (Keek et al. 2009). Furthermore, Keek et al. found that the frequency drift of the QPOs before X-ray bursts may be due to the cooling process of the layer where the mHz QPOs occur. Keek et al. (2014) investigated the influence of the fuel composition and nuclear reaction rates on the mHz QPOs, and concluded that no allowed variation in the composition and the reaction rate is able to trigger the mHz QPOs at the observed accretion rates.

Lyu et al. (2015) found that there was no significant correlation between the frequency of the mHz QPOs and the temperature of the neutron-star surface in 4U 1636–53, which is different from theoretical predictions. Furthermore, they found that seven X-ray bursts associated with mHz QPOs in this source were bright, energetic, and short, indicating a potential connection between the mHz QPOs and He-rich X-ray bursts. Lyu et al. (2016) investigated the convexity of 39 type I X-ray bursts associated with mHz QPOs in 4U 1636–53 and found that all the bursts show positive convexity. This finding suggests that these mHz QPOs and the associated bursts may originate at the equator of the neutron-star surface.

In this work we investigate the properties of mHz QPOs detected with the *Rossi X-ray Timing Explorer* (*RXTE*) in the LMXB 4U 1636–53 and, for the first time, we carry out a systematic study of their frequency and amplitude. Furthermore, we explore the connection between the frequency, amplitude, count rate, and position of the source in the color-color diagram, which provides useful information for studying the origin of the mHz QPOs. In Section 2 we describe the observations and data analysis used in this work, and in Section 3 we present our main results. Finally, we discuss the results in the framework of the marginally stable nuclear burning model in Section 4.

## 2. Observations and Data Reduction

We analyzed the observations with the mHz QPOs reported in Lyu et al. (2016) in 4U 1636–53 using the Proportional Counter Array (PCA; Jahoda et al. 2006) on board the *RXTE*. An *RXTE* observation typically covers 1–5 consecutive 90 min satellite orbits, which usually contain between 1 and 5 ks of useful data separated by 1–4 ks data gaps. We extracted two event mode PCA light curves of 1 s resolution in the  $\sim 2$ –4.5 keV range (where the mHz QPOs are the strongest; see Altamirano et al. 2008b), with one light curve from all available proportional counter units (PCUs) and the other one from PCU2 only. Bursts and instrumental dropouts were removed.

Since mHz QPOs are not always present in the whole observation, we further divided each light curve extracted from all available PCUs into a series of independent 700 s intervals, and used Lomb–Scargle periodograms (Lomb 1976; Scargle 1982) to check whether there is a significant QPO in each interval. We found that, in some cases, although there is a more

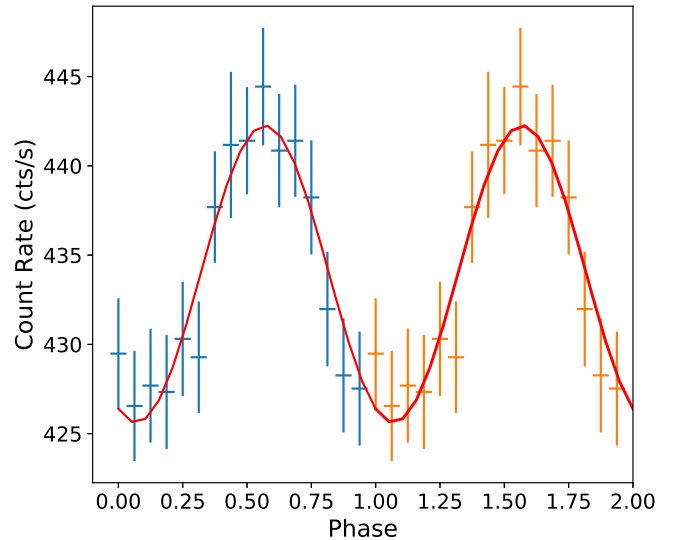


**Figure 1.** Fitting example of the folded light curve extracted from an *RXTE*/PCA data interval (14,000–14,700 s in dc7ff0-dc867e5 in 50030-02-10-00) of 4U 1636–53. The red line represents the best-fitting result with the model consisting of a constant plus a sine function. Here we show the data and the model curve for two periods for clarity.

than  $3\sigma$  significant QPO in an observation, the QPO is less than  $3\sigma$  significant in some of the 700 s intervals in that observation. This can occur either because the QPO is indeed not present during those intervals, or because the amplitude of the QPO or the source count rate decreased slightly in that interval and the QPO dropped below the  $3\sigma$  detection level. Besides, in some cases, random fluctuations may marginally reach the  $3\sigma$  significance level, likely where the count rate increases. Therefore, we consider only those intervals where either: (i) there are at least two consecutive 700 s intervals in which the QPO is more than  $3\sigma$  significant, or (ii) if there is only one 700 s interval and the QPO there is more than  $3\sigma$  significant, then there must be a harmonic at twice the QPO frequency.

For each 700 s interval with a mHz QPO, we then folded the corresponding 700 s light curve from all available PCUs at the period derived from the frequency measured in the Lomb–Scargle periodogram. We took the frequency at which the power is the strongest in the periodogram to be the frequency of the mHz QPO in each interval. We used the half width at half maximum as an indication of the error of the frequency of the QPOs. We used the `fool` fold to fold the light curve and normalized the folded light curve to counts  $s^{-1}$ , with the error bars evaluated by error propagation. We then fitted each folded light curve with a constant plus a sine function to measure the fractional rms amplitude of the mHz QPO (see Figure 1 for example). To estimate the contribution of background to the total count rate, we used the tool `pcabackest` to create an estimated PCA background light curve in the  $\sim 2$ –4.5 keV and calculated the average count rate. We then calculated the fractional rms amplitude of the mHz QPO using the formula  $rms = A/[\sqrt{2} * (C - B)]$ , where  $A$  is the amplitude of the sine function,  $C$  is the value of the constant component, and  $B$  is the count rate of the estimated background. Furthermore, we calculated the absolute RMS amplitude of the mHz QPOs detected by PCU2 detector,  $RMS = rms \times R$ , where  $R$  is the count rate from the PCU2 detector.

To explore the possible link between the properties of the mHz QPOs and the different accretion states of the source, we

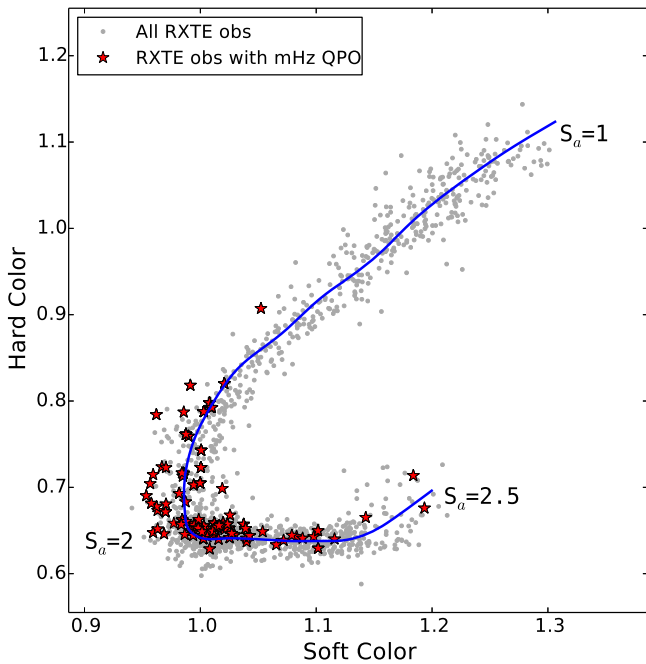


**Figure 2.** Color-color diagram of 4U 1636–53 using all *RXTE* observations. Each gray point represents the averaged Crab-normalized colors (see Zhang et al. 2011 for details) of a single *RXTE* observation. The red stars mark the position of the observations where mHz QPOs are detected. The position of the source in the diagram is parameterized by the length of the blue solid curve  $S_a$  (see also Zhang et al. 2011).

constructed the color-color diagram and further traced the evolution of the frequency and amplitude of the mHz QPO as function of the quantity  $S_a$  (see below). We used the 16 s time-resolution Standard-2 data available from the *RXTE*/PCA to calculate two X-ray colors. We defined the soft color as the count rate in the 3.5–6.0 keV band divided by that in the 2.0–3.5 keV band, and the hard color as the count rate in the 9.7–16.0 keV band divided by that in the 6.0–9.7 keV band. The colors were normalized to those of the Crab Nebula in observations taken close in time to those of 4U 1636–53 (see Altamirano et al. 2008a; Zhang et al. 2009, for more details). We defined the  $S_a$  quantity on the basis of the color-color diagram of the source as in Zhang et al. (2011), with the  $S_a$  length being normalized to the distance between  $S_a = 1$  at the top right-hand vertex and  $S_a = 2$  at the bottom left-hand vertex of the color-color diagram. The  $S_a$  value of each particular observation was then assigned to be the same as the value of the point closest to that observation along the  $S_a$  curve. The quantity  $S_a$  is usually assumed to be an increasing function of mass accretion rate (Hasinger & van der Klis 1989; Zhang et al. 2011).

### 3. Results

In total, we detected mHz QPOs in 374 individual 700 s intervals. In Figure 2 we show the color-color diagram for all *RXTE* observations of 4U 1636–53. We find that the observations with mHz QPOs are either in the transitional spectral state or in the soft spectral state, with most of them clustering around the vertex between the two branches, at  $S_a \sim 2$ . The hard color of the observations with mHz QPOs is less than  $\sim 0.9$ , suggesting that the mHz QPOs do not appear in the hard spectral state.

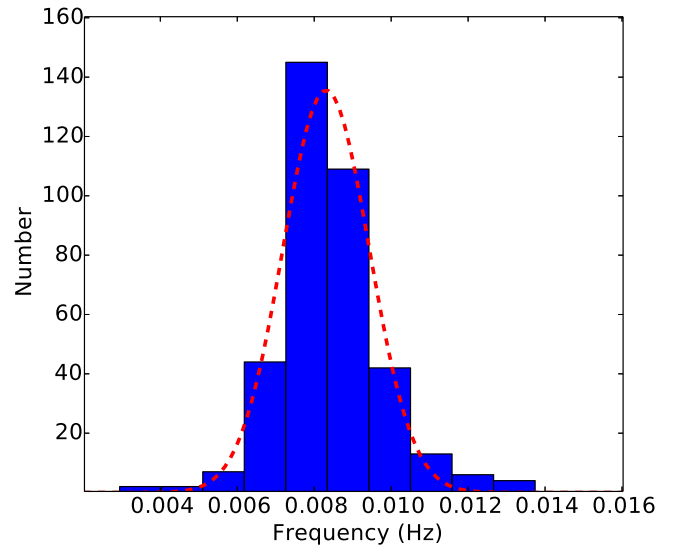


**Figure 3.** Distribution of the frequency of the mHz QPOs in each 700 s interval in 4U 1636–53. The red dashed line in the plot corresponds to the best-fitting Gaussian curve to the histogram.

In Figure 3 we show the distribution of the frequency of the mHz QPOs in 4U 1636–53. The distribution is symmetric, ranging from  $\sim 3$  mHz to  $\sim 14$  mHz. As shown in the plot, the distribution can be well described by a Gaussian function with a mean frequency of  $8.31 \pm 0.06$  mHz (all errors are at 68% confidence level) and a standard deviation of  $1.12 \pm 0.05$  mHz. We show the distribution of the fractional rms amplitude and absolute RMS amplitude of the mHz QPOs in Figure 4. The fractional rms amplitude ranges from  $\sim 0.5\%$  to  $\sim 4.5\%$ , with most of the values clustering between 0.5% and 2.5%. The distribution of the absolute RMS amplitude of the mHz QPOs is symmetric; if we fit a Gaussian function to these data the best-fitting average value and the standard deviation are  $1.41 \pm 0.02$  counts  $s^{-1}$  and  $0.29 \pm 0.01$  counts  $s^{-1}$ , respectively.

In Figures 5 and 6 we plot, respectively, the frequency and the fractional and absolute RMS amplitudes of the mHz QPOs in 4U 1636–53 as a function of the parameter  $S_a$ . There is no clear correlation between the QPO frequency and  $S_a$  (correlation coefficient =  $-0.4$ ), with most of the data in the figure clustering in the  $S_a$  range 2.0–2.2. The absolute RMS amplitude remains more or less constant as  $S_a$  increases; if we fit a power-law function to these data the best-fitting power-law index is  $\sim 0.01 \pm 0.10$ . In contrast, there is a significant anti-correlation between the fractional rms amplitude and  $S_a$  (correlation coefficient =  $-0.8$ ). The fractional rms amplitude decreases as  $S_a$  increases up to  $S_a \sim 2.2$ , and then it remains more or less constant when  $S_a$  increases above  $\sim 2.2$ .

In Figure 7 we show the relation between the frequency and the fractional rms amplitude of the mHz QPOs in 4U 1636–53. We find no clear correlation between them. The correlation coefficient for the data in this plot is  $\sim 0.2$ , indicating that these two quantities are not significantly correlated.

In Figure 8 we show the fractional rms amplitude of the mHz QPOs in 4U 1636–53 versus the count rate of the PCU2 detector below  $\sim 5$  keV. We find that there is a significant anti-correlation between the rate and the fractional rms amplitude. As the count rate increases, the fractional rms amplitude drops rapidly when the count rate is below  $\sim 100$  counts  $s^{-1}$ , and then it decreases much more slowly when the count rate is larger than 100 counts  $s^{-1}$ . The anti-correlation between the rate and

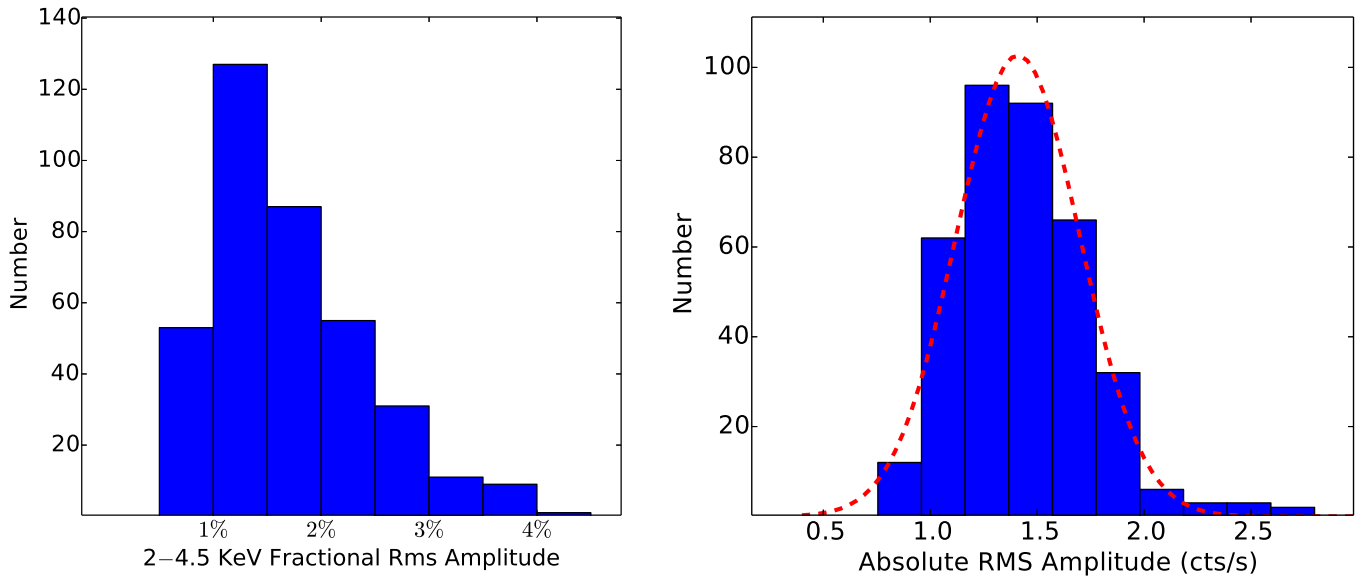


**Figure 4.** Distribution of the fractional rms amplitude and absolute RMS amplitude of the mHz QPOs in each 700 s interval in 4U 1636–53. The red dashed line in the right plot corresponds to the best-fitting Gaussian curve to the histogram. The absolute RMS amplitude is measured with the PCU2 detector in 2–4.5 keV range.

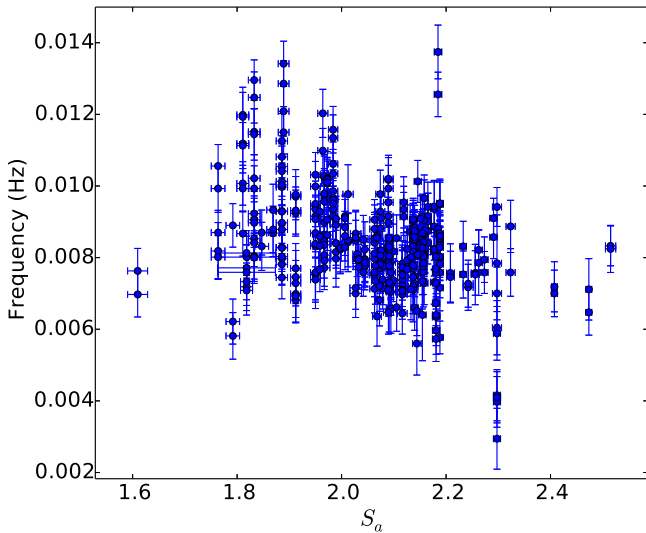


**Figure 5.** Frequency of the mHz QPOs vs.  $S_a$  in 4U 1636–53. Each data point in the plot corresponds to a 700 s interval.

the fractional rms amplitude can be well fitted by a power-law relation with a power-law index<sup>8</sup>  $-0.89 \pm 0.02$ .

#### 4. Discussion

We systematically investigated the properties of the mHz QPOs in 4U 1636–53 using *RXTE* observations. We found that the mHz QPOs are present only in the soft spectral state or the transitional state between the soft and the hard state. We found no clear correlation between the frequency and the fractional rms amplitude of the mHz QPOs. More importantly, the absolute RMS amplitude of the mHz QPOs in 4U 1636–53 remains constant as  $S_a$  increases, as the source gradually moves to the soft state. Furthermore, we found an anti-correlation

<sup>8</sup> The index may be slightly overestimated due to the fact that the fractional rms amplitude of the QPOs decreases rapidly at high count rate and, since the significance of a QPO scales with the square of the fractional rms amplitude (van der Klis 1997), we tend to miss mHz QPOs that are marginally significant at these count rates in Figure 8.

between the fractional rms amplitude and the source count rate below  $\sim 5$  keV.

The finding that mHz QPOs are not present in the hard spectral state suggests that they can be triggered only when the mass accretion rate exceeds a certain threshold value; this is consistent with the model of Heger et al. (2007). The critical accretion rate at which mHz QPOs are triggered in Heger et al. is very close to the Eddington accretion rate, significantly higher than the averaged global accretion rate deduced from X-ray luminosity. Moreover, the model of Heger et al. predicts a very narrow local accretion rate range where mHz QPOs occur, whereas we find them over a relatively wide  $S_a$  range, from  $\sim 1.6$  to 2.5 of the full range of  $S_a$  values (see Figures 5 and 6). If  $S_a$  is indeed correlated to  $\dot{M}$  (Hasinger & van der Klis 1989; Zhang et al. 2011), this result implies that in 4U 1636–53 either the mHz QPOs exist over a wide range of  $\dot{M}$ , in contradiction to the model or, in the region of the color–color diagram in which the mHz QPOs are detected,  $\dot{M}$  is not strongly correlated to  $S_a$ . On the other hand, when the mHz QPOs are present the soft X-ray intensity changes by a factor of  $\sim 4$  (see Figure 8), which favors the idea that in 4U 1636–53, when the mHz QPOs are present,  $\dot{M}$  changes by a large factor. A scenario that can well bridge the accretion rate difference between models and observations is that the mHz QPOs are triggered by the local accretion rate around the equator of the neutron-star surface instead of the global accretion rate of the whole neutron-star surface (Heger et al. 2007; Altamirano et al. 2008b; Lyu et al. 2016).

Revnivtsev et al. (2001) investigated the properties of the mHz QPOs and found that their centroid frequency in the  $\sim 2$ –5 keV energy range is  $\sim 7$ –9 mHz. Altamirano et al. (2008b) found that their frequency ( $\sim 2$ –5 keV) in 4U 1636–53 ranges between  $\sim 7$ –14 mHz. The frequency range of the mHz QPOs derived in this work is  $\sim 3$ –14 mHz. We measured their average frequency at a much smaller time interval (700 s) compared with previous authors, and this may account for the relatively wider frequency range measured in this work. For the same reason, the range of the fractional rms amplitude of the mHz QPOs that we found here is also somewhat larger than the fractional rms amplitude range

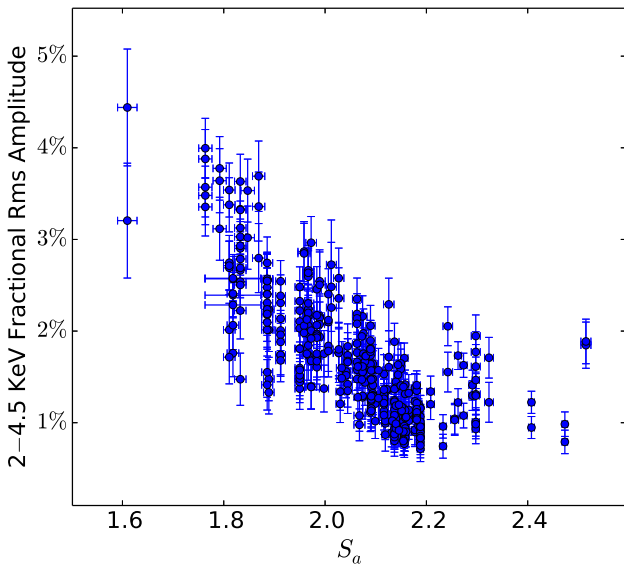


**Figure 6.** Fractional rms and absolute RMS amplitude of mHz QPOs vs.  $S_a$  in 4U 1636–53. Each data point in the plot corresponds to a 700 s interval. The absolute RMS amplitude is measured with the PCU2 detector in 2–4.5 keV range.

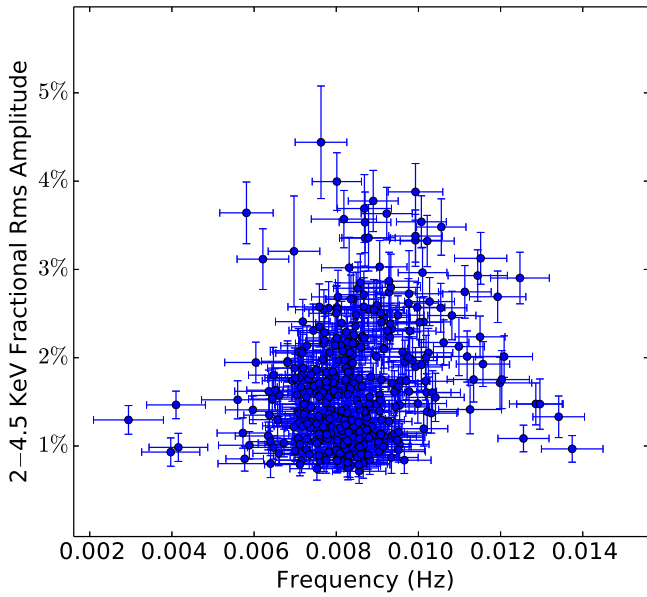
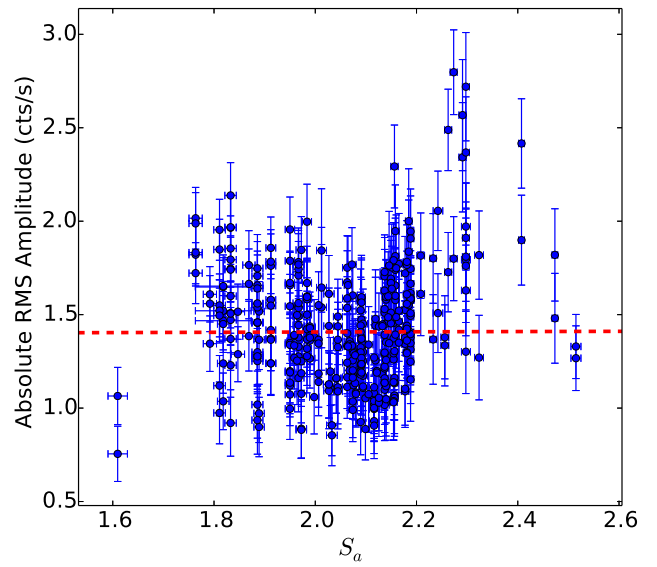


**Figure 7.** Fractional rms amplitude of the mHz QPOs vs. the frequency of the mHz QPOs in 4U 1636–53. Each data point in the plot corresponds to a 700 s interval.

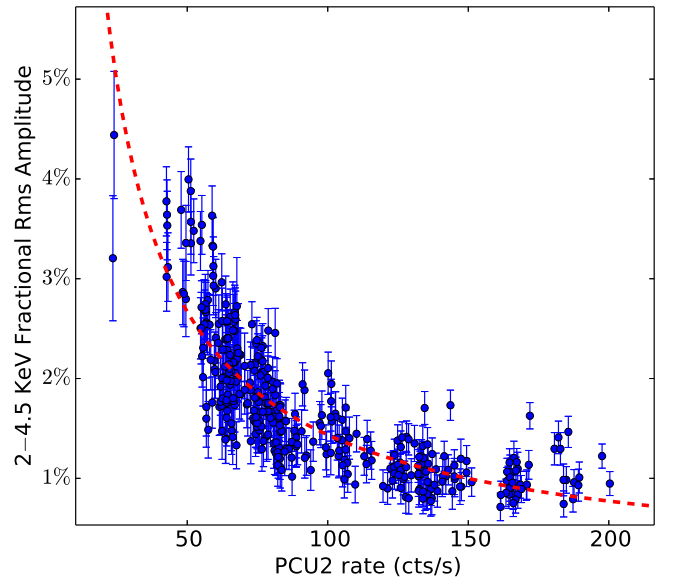


**Figure 8.** Fractional rms amplitude of the mHz QPOs as a function of the count rate of the PCU2 light curve ( $< \sim 5$  keV) in 4U 1636–53. The red dashed lines in the plots correspond to the best-fitting power-law model to the data. Each data point in the plot corresponds to a 700 s interval.

( $\sim 0.6\%$ – $2\%$ ) reported in Revnivtsev et al. (2001). The fractional rms amplitude of the mHz QPOs in this work can reach up to  $\sim 4\%$  in 4U 1636–53.

A linear relationship between the absolute RMS amplitude of short-term variability and flux variations on longer timescales was first discovered in X-ray binary systems as well as in active galactic nuclei (Uttley & McHardy 2001). Further analysis showed that this linear RMS–flux relation occurs on all measured timescales (Uttley et al. 2005). This RMS–flux relation in accreting systems is likely linked to the accretion flow itself, with variations arising from fluctuations in the accretion rate at different radii, which propagate through the flow so that variability is coupled together over a broad range of timescales (Lyubarskii 1997; King et al. 2004; Arévalo & Uttley 2006; Ingram & van der Klis 2013; Cowperthwaite & Reynolds 2014; Scaringi 2014; Hogg & Reynolds 2016). In

this work we found an anti-correlation between the fractional rms amplitude of the mHz QPOs and the count rate below 5 keV in 4U 1636–53. The derived power-law index ( $\sim -0.9$ ) indicates that there is no significant correlation between the absolute RMS amplitude of the mHz QPOs and the soft count rate in 4U 1636–53, different from the linear RMS–flux relationship described above. This difference indicates that the relation in this work is likely to have a different physical origin compared with that of the linear relationship described above, further supporting the idea that the mHz QPOs likely originate from the neutron-star surface. However, The physical mechanism behind the relation in this work is still unknown. Keek et al. (2009) simulated the nuclear burning process on the neutron-star surface and found that oscillations in their simulations generally exhibit larger amplitudes as the heat flux

from the neutron-star crust decreases. If the heat flux is proportional to the temperature of the neutron-star surface, and hence correlated with the number of soft photons from the neutron star, then there should be an anti-correlation between the amplitude of the mHz QPOs and the count rate in the soft band.

The independence of the absolute RMS amplitude with the parameter  $S_a$  suggests that the disappearance of the mHz QPOs should be a very quick process. Simulations in Heger et al. (2007) indicate that marginally stable nuclear burning switches to stable/unstable burning as the accretion rate further increases/decreases, leading to the disappearance of the mHz QPOs. If the absolute RMS amplitude remains constant when  $S_a$  changes, then this switch should be suddenly triggered and then rapidly finished, consistent with the observational feature that the mHz QPOs suddenly disappear when there is a type I burst.

This research has made use of data obtained from the High Energy Astrophysics Science Archive Research Center (HEASARC), provided by NASA's Goddard Space Flight Center. This research made use of NASA's Astrophysics Data System. M.L. is supported by National Natural Science Foundation of China (grant No.11803025), the Hunan Provincial Natural Science Foundation (grant No. 2018JJ3483) and Hunan Education Department Foundation (grant No. 17C1520). D.A. acknowledges support from the Royal Society. G.B. acknowledges funding support from the National Natural Science Foundation of China (NSFC) under grant Nos. U1838116 and the CAS Pioneer Hundred Talent Program Y7CZ181002. G.C.M. thanks the Royal Society International Exchanges program for their support. G.C.M. was partially supported by PIP 0102 (CONICET) and received financial support from PICT-2017-2865 (ANPCyT).

## ORCID iDs

Guobao Zhang  <https://orcid.org/0000-0001-8630-5435>

## References

- Altamirano, D., van der Klis, M., Méndez, M., et al. 2008a, *ApJ*, **685**, 436  
 Altamirano, D., van der Klis, M., Wijnands, R., & Cumming, A. 2008b, *ApJL*, **673**, L35  
 Arévalo, P., & Uttley, P. 2006, *MNRAS*, **367**, 801  
 Chakraborty, M., & Bhattacharyya, S. 2011, *ApJL*, **730**, L23  
 Cowperthwaite, P. S., & Reynolds, C. S. 2014, *ApJ*, **791**, 126  
 Hasinger, G., & van der Klis, M. 1989, *A&A*, **225**, 79  
 Heger, A., Cumming, A., & Woosley, S. E. 2007, *ApJ*, **665**, 1311  
 Hogg, J. D., & Reynolds, C. S. 2016, *ApJ*, **826**, 40  
 Ingram, A., & van der Klis, M. 2013, *MNRAS*, **434**, 1476  
 Jahoda, K., Markwardt, C. B., Radeva, Y., et al. 2006, *ApJS*, **163**, 401  
 Keek, L., Cyburt, R. H., & Heger, A. 2014, *ApJ*, **787**, 101  
 Keek, L., Langer, N., & in't Zand, J. J. M. 2009, *A&A*, **502**, 871  
 King, A. R., Pringle, J. E., West, R. G., & Livio, M. 2004, *MNRAS*, **348**, 111  
 Linares, M., Altamirano, D., Chakraborty, D., Cumming, A., & Keek, L. 2012, *ApJ*, **748**, 82  
 Linares, M., Altamirano, D., Watts, A., et al. 2010, *ATel*, **2958**, 1  
 Lomb, N. R. 1976, *Ap&SS*, **39**, 447  
 Lyu, M., Méndez, M., Altamirano, D., & Zhang, G. 2016, *MNRAS*, **463**, 2358  
 Lyu, M., Méndez, M., Zhang, G., & Keek, L. 2015, *MNRAS*, **454**, 541  
 Lyubarskii, Y. E. 1997, *MNRAS*, **292**, 679  
 Mancuso, G. C., Altamirano, D., García, F., et al. 2019, *MNRAS*, **486**, 74  
 Revnivtsev, M., Churazov, E., Gilfanov, M., & Sunyaev, R. 2001, *A&A*, **372**, 138  
 Scargle, J. D. 1982, *ApJ*, **263**, 835  
 Scaringi, S. 2014, *MNRAS*, **438**, 1233  
 Stiele, H., Yu, W., & Kong, A. K. H. 2016, *ApJ*, **831**, 34  
 Strohmayer, T. E., Gendreau, K. C., Altamirano, D., et al. 2018, *ApJ*, **865**, 63  
 Uttley, P., & McHardy, I. M. 2001, *MNRAS*, **323**, L26  
 Uttley, P., McHardy, I. M., & Vaughan, S. 2005, *MNRAS*, **359**, 345  
 van der Klis, M. 1997, in *Astronomical Time Series*, ed. D. Maoz, A. Sternberg, & E. M. Liebowitz (Dordrecht: Kluwer)  
 Yu, W., & van der Klis, M. 2002, *ApJL*, **567**, L67  
 Zhang, G., Méndez, M., & Altamirano, D. 2011, *MNRAS*, **413**, 1913  
 Zhang, G., Méndez, M., Altamirano, D., Belloni, T. M., & Homan, J. 2009, *MNRAS*, **398**, 368